COMPARISON OF IN SITU AND SATELLITE-DERIVED CLOUD PROPERTIES DURING SUCCESS

David F. Young, Patrick Minnis
NASA Langley Research Center
Hampton, Virginia

Darrel Baumgardner
National Center for Atmospheric Research
Boulder Colorado

H. Gerber
Gerber Scientific Inc.
Reston Virginia

Submitted to *Geophysical Research Letters* SUCCESS Special Issue

June 1997

Abstract.
The validation of cloud microphysical properties derived from satellite data with in situ observations is generally difficult due to the horizontal, vertical and temporal variability of observed clouds. The SUCCESS mission has provided an excellent opportunity for such a comparison. Two missions during SUCCESS concentrated on orographic wave clouds that exhibited relative spatial and temporal homogeneity. A comparison has been made of effective ice particle diameters derived from multi-spectral satellite data with in situ measurements from the MASP and PVM instruments aboard the DC-8 aircraft. For both days, the satellite-derived effective diameters fall well within the bounds of the in situ data.

Introduction

The microphysical properties of a wide array of cirrus clouds were sampled in situ during the spring 1996 NASA Subsonic Clouds and Contrails Effects Special Study (SUCCESS) conducted under the auspices of the NASA Subsonic Assessment Program and First ISCCP Regional Experiment (FIRE). These measurements provide the resources for addressing one of FIRE's objectives, the validation of satellite-retrieved microphysical properties. A methodology (Minnis et al., 1995) and models of cloud optical properties (Minnis et al., 1997a) have recently been developed for retrieving cloud microphysical properties from all types of clouds using multispectral data from the Geostationary Operational Environmental Satellite (GOES) multispectral imager, the NOAA Advanced Very High Resolution Radiometer (AVHRR), and other similar instruments. This paper uses a subset of the SUCCESS data to begin the process of validating the retrieval methodology and models.

Two wave cloud cases are the focus of this investigation because they were extensively sampled in situ during SUCCESS near the overpass of NOAA-14 and showed more uniformity than most cirrus clouds. Model studies (Eric Jensen, personal communication) suggest that wave clouds tend to be vertically uniform in particle size, thereby minimizing one of the factors, vertical inhomogeneity, that complicates the comparison of in situ and satellite retrievals. Thus, it should be possible to draw more definitive conclusions concerning the validity of the satellite results for wave clouds.

Data and Methodology

The in situ data were collected with the multi-angle aerosol spectrometer probe (MASP; Baumgardner et al., 1995; Baumgardner et al., 1997) and the particulate volume monitor (PVM; Gerber et al., 1994; Gerber et al., 1997) flown on the NASA DC-8 during SUCCESS. These instruments measure the ice particles optically and assume spherical particles when determining the particle sizes. The size range of the MASP extends from 0.3 μm to 40 μm. The PVM size range extends to 50 μm. For this study, estimates of effective diameter from these instruments are made once every 5 seconds from MASP and once every second for PVM.

Both 1-km and 4-km NOAA-14 AVHRR and the 4-km, GOES-8 imager data were analyzed pixel by pixel in a box containing the selected DC-8 flight tracks for the two cases, April 30 and May 2, 1996. The AVHRR visible (VIS; 0.65 μm), solar infrared (SI; 3.7 μm), and infrared (IR; 10.8 μm) data and the nearest coincident GOES VIS, SI (3.9 μm), and IR (10.9 μm) pixels were analyzed with the VIS-SI-IR technique (VIST; Minnis et al., 1995) to derive effective ice particle diameter D_e, VIS optical depth τ, and cloud temperature T_c. The VIST uses an iterative technique to simultaneously determine values for each parameter given the observed VIS reflectance ρ, and the SI and IR brightness temperatures and estimates of the clear-sky reflectance ρ_s, and SI and IR clear-sky brightness temperatures T_{SI} and T_{cs}. Temperatures and reflectances for a range of particle sizes and optical depths are computed for the given solar zenith, viewing zenith, and relative azimuth angles, θ_o, θ, and ψ, respectively, using the cloud emittance and reflectance parameterizations of Minnis et al. (1997a) and a VIS surface-atmosphere-cloud reflectance parameterization (Minnis et al., 1993). The cloud

parameters are determined by iteratively solving for the best match between the observed and modeled temperatures and reflectances.

The reflectances for the AVHRR and GOES are computed as

$$\rho = \frac{\pi L_V}{526.9 \cos\theta_0 \, \delta(d)}, \qquad (1)$$

where the observed radiance is $L_v = a_0 + a_1 CT$, CT is the 10-bit count, d is the day of the year, and δ is the Earth-Sun distance correction factor. The calibration coefficients a_0 and a_1 are -4.93 and 0.120 for AVHRR and -19.2 and 0.674 for GOES-8, respectively. The nominal satellite calibrations were used to convert counts to temperatures. The reflected solar component was determined using SI solar constant values that are equivalent to T_{SI} = 357.3K and 338.0K for AVHRR and GOES-8, respectively. Soundings from National Weather Service stations at Albuquerque, NM (April 30) and Denver CO (May 2) from 1200 UTC were used to convert temperature to altitude and adjust for the effects of humidity on the IR radiances.

Effective ice particle diameter for the particle distributions used in the VIST models are calculated by:

$$D_e = \frac{\int_{L_1}^{L_2} D^2 LN(L) dL}{\int_{L_1}^{L_2} DLN(L) dL} \qquad (2)$$

where L is the particle length, D is the particle width, and N is the normalized number of particles in a size bin. Effective diameters are calculated from the in situ data using equation (2) and assuming spherical particles ($D = L$).

Results and Discussion

May 2, 1996. A wave cloud located east of the Front Range of the Rocky Mountains was sampled by the NASA DC-8 between 19.6 and 21.8 UTC, 2 May 1996. This cloud formed around 19 UTC and persisted past 22 UTC. Figure 1 shows the location of this cloud in the NOAA-14 IR image from 20.56 UTC. The box in each image indicates the area analyzed by VIST using data from both AVHRR and GOES. Figure 1b also shows the DC-8 flight track for 20.37 - 20.65 UTC.

The northeast-southwest leg of the DC-8 flight between the times of 20.55 - 20.61 UTC provides excellent temporal coordination with the NOAA-14 overpass time of 20.56. Essentially the same area was sampled earlier between 20.43 - 20.49 on the same path while the aircraft traveled to the northeast.

During these passes the DC-8 flew near the top of the cloud (~11.8 km) at an ambient temperature of 209 K. ER-2 lidar data indicate that this cloud extended vertically from 12 km to at least 9.8 km (Spinhirne et al., 1997). The true bottom of the cloud is unknown since the lidar signal was attenuated by the cloud. Although this was an optically thick cloud, no temperatures below 219 K were observed in the 1 km resolution AVHRR data. This suggests that the majority of the cloud mass is beneath the DC-8 flight level and that the satellite is observing properties from a lower portion of the cloud.

Cloud properties derived from the 1-km resolution AVHRR data are shown in Figure 2 for the area in the box in Figure 1. Pixels classified by VIST as clear are indicated in black. Gray pixels indicate data that cannot be fit with consistency by the VIST algorithm and are reported as "no retrieval." In order to eliminate lower clouds in this region from our comparisons, the area of the wave cloud is defined as the portion of these fields where the emittance exceeds 0.8 and the retrieved cloud temperature is less than 250 K. The central portion of the cloud is nearly thermally black (cloud emittances, $\varepsilon > 0.95$). The visible optical depth ranges from 4 - 20 throughout most of the cloud. The particle sizes are consistently small, ranging between 10 - 25 μm in the main body of the cloud.

This scene was also analyzed using the 4-km AVHRR data and the GOES data from 20.75 UTC. Since these data have degraded resolution compared with the 1 km AVHRR, care must be taken in comparisons to avoid cloud edge contamination. All comparisons were performed using only those pixels with retrieved emittances greater than 0.85. These results are summarized in Table 1.

The agreement between ice particle diameters retrieved from the two satellites is quite good. Particle sizes range from 17.9 ± 2.1 from GOES to 19.7 ± 3.9 for the lower resolution AVHRR. Also, the data indicate that particle sizes sampled along the flight track are representative of the cloud as a whole. There is, however, some discrepancy among the retrieved values of optical depth and cloud temperature. The optical depth comparison can be difficult when using data with varying spatial resolution. The comparison is much better if the 4-km AVHRR and the GOES data are restricted to pixels with cloud emittance greater than 0.95. For these data, the AVHRR optical depth increases to 9.1, which is in much better agreement with the 1-km data. The GOES optical depth also increases (to 5.5), but not as much. This may indicate some inconsistency in the relative visible calibrations, although the GOES calibration was based on coincident April 1996 GOES and AVHRR data. The temperatures are all consistently much higher than the temperature at the DC-8 flight level. This is caused largely by the satellite seeing the optical center of the cloud. However, the overall retrieved cloud temperatures may also be biased too high due to the effects of partial cloudiness near the cloud edges.

Data from the PVM and MASP instruments were averaged for the 20.55 - 20.61 UTC time period and compared with a two-pixel-wide swath of satellite data taken along the flight track. This portion of the DC-8 track is indicated by the black line in Figure 2. For this region, the VIST retrieves particles with D_e = 18.7 ± 2.3 μm. The MASP data averages to 18.7 ± 1.9 μm, while the PVM measured 11.8 ± 1.6 μm. During the earlier flight leg (20.43 - 20.49 UTC)

the MASP and PVM measured effective diameters of 19.6 μm and 12.7, respectively. The frequency distributions of D_e are compared in Figure 3. The in situ distribution shows the time variability of D_e , while the spread in the VIST data is indicative of spatial variation along the track at 20.56. The VIST and MASP distributions are remarkably similar. The PVM data show a similar relative distribution, but the mean diameter is somewhat lower. Small ice crystals such as these are not unusual for wave clouds of this type, so it is not obvious which in situ data set represents the best estimate of the actual particles. Additional studies are needed to reconcile the differences in these in situ measurements (see Gerber et al., 1997; Jensen et al., 1997). However, the satellite-derived values of effective particle size are well within the bounds of the in situ observations.

April 30, 1996. A wave cloud located east of the Rocky Mountains in New Mexico was sampled by the DC-8 between 19.3 and 21.3 UTC, April 30, 1996. The DC-8 flew numerous passes through the cloud at an altitude of 8.5 - 9.0 km at an ambient temperature of ~236 K. Figure 4 shows the NOAA-14 AVHRR IR image from 20.92 UTC. This relatively isolated wave cloud consisted of several sections over sloping terrain having a steep gradient in surface temperature. The wide variation in the surface background and the cloud create a more difficult situation for deriving cloud properties using satellite data. In addition, the satellite overpass time of 20.92 UTC occurs in the middle of a time period when the DC-8 was out of the cloud (20.74 - 21.2 UTC). Therefore, comparisons for this day are not as direct as those for May 2.

Table 2 summarizes the results of VIST retrievals. The variable nature of this cloud is apparent in the increase in the standard deviations of the retrieved particle diameters. The results for the 4-km data are also much more sensitive to changes in the cloud emittance cut-off used to define the central portion of the cloud. Partial cloudiness near cloud edges generally causes an increase in the retrieved particle sizes and in the derived cloud temperature, as is seen here. Using a more stringent condition of emittance greater than 0.90 causes the satellites retrievals to be more consistent. In contrast with the May 2 data, the optical depths derived from GOES and AVHRR are roughly equivalent when only the highest emittance data are considered. Once again, the cloud temperatures appear to be quite warm compared with the cloud top temperature as the satellite data are seeing further into the cloud.

A comparison of the distribution of particle sizes derived from VIST, MASP, and PVM is shown in Figure 5. The in situ data are from the time period 20.0 - 20.8 UTC and the satellite values are from the 1-km AVHRR data at 20.92 UTC. Although the satellite data demonstrates greater variability, the three data sets agree well with D_e = 19.9 ± 5.4 μm, 16.2 ± 3.0 μm, and 17.1 ± 2.9 μm for VIST, MASP, and PVM, respectively. Table 2 also includes mean particle sizes for MASP and PVM for the later time period of 20.8 - 21.5 UTC. The PVM data indicates less variable particle sizes between the two times than the MASP data.

Conclusions

Wave cloud properties have been derived from satellite data using the VIST multi-spectral technique. In general, there is very good agreement between the effective ice particle diameters and cloud temperatures derived from GOES and AVHRR data, even when viewing conditions vary. Derived optical depths show less consistency, possibly due to calibration errors. Derived cloud temperatures are consistently higher than the ambient temperature of the in situ instruments since the DC-8 flew near cloud top and the location of the cloud radiating center is well below the top in cirrus clouds. Some additional bias in temperature may be due to the effects of partial cloudiness near cloud edges. This same effect can also cause an overestimate in the particle sizes for the lower resolution data.

A comparison of the distribution of effective particle diameters with in situ measurements shows that the satellite-derived diameters are quite reasonable. For the May 2 case when there is almost complete temporal and spatial simultaneity, the agreement with the MASP data is excellent. The cloud variability and lack of temporal simultaneity of the April 30 case causes

more noise in the comparisons. On this day, the VIST results compare best with the PVM data, although all three data sets are in fairly good agreement. Overall, the uncertainty in the satellite retrieved particle sizes appears to span the range of the in situ data measured by the different instruments, providing a degree of confidence in the VIST retrievals for small ice-crystal clouds.

References

Baumgardner, D., J.E. Dye, B. Gandrud, R.G. Knollenberg, The multiangle aerosol spectrometer probe: A new instrument for airborne particle research, *Proc. AMS 11th Symp. on Boundary Layers and Turbulence*, March 27-31, 1995, Charlotte, N.C., 1995

Baumgardner, D., The microphysical and optical properties of contrail and wave cloud particles, Submitted to *Geophys. Res. Lettr.*, this issue, 1997

Gerber, H., B. G. Arends, and S. A. Ackerman, New microphysiics sensor for aircraft use, *Atmos. Res.*, 32, 235-252, 1994.

Gerber, H.,, C. H. Twohy, B. Gandrud, A. J. Heymsfield, P. J. DeMott, and D. C. Rogers, Measurement of wave-cloud microphysics with two new aircraft probes, Submitted to *Geophys. Res. Lettr.*, this issue, 1997.

Jensen, E. J., O. B. Toon, A. Tabazadeh, G. S. Sache, B. E. Anderson, K. R. Chan, D. Baumgardner, C. H. Twohy, B. Gandrud, A. J. Heymsfield, J. Hallett, and B. L. Gary, Ice nucleation processes in upper tropospheric wave-clouds observed during SUCCESS, Submitted to *Geophys. Res. Lettr.*, this issue, 1997.

Minnis, P., J. K. Ayers, L. Nguyen, W. L. Smith, Jr., and R. Palikonda, Calibration of satellite visible and infraredsensors for field experiments and the ARM Program. Submitted to *J. Atmos. Oceanic Tech.*, 1997a.

Minnis, P., D. P. Kratz, J. A. Coakley, Jr., M. D. King, R. Arduini, D. P. Garber, P. W. Heck, S. Mayor, W. L. Smith, Jr., and D. F. Young, Cloud optical property retrieval (Subsystem 4.3). "Clouds and the Earth's Radiant Energy System (CERES) Algorithm Theoretical Basis Document, Volume III: Cloud Analyses and Radiance Inversions (Subsystem 4)", *NASA RP 1376 Vol. 3*, edited by CERES Science Team, pp. 135-176, December, 1995.

Minnis, P., D. P. Garber, D. F. Young, R. F. Arduini, and Y. Takano, Parameterizations of reflectance and effective emittance for satellite remote sensing of cloud properties. Submitted to *J. Atmos. Sci.*, 1997b.

Spinhirne, J., W. Hart, and D. Duda, Remote sensing observation of contrail structure and microphysics, Submitted to *Geophys. Res. Lettr.*, this issue, 1997.

Table 1. Summary of derived cloud properties from wave cloud, May 2, 1996.

Data	D_e (μm)	$\sigma(D_e)$ (μm)	Optical Depth	Cloud Temperature (K)	Cloud Center Height (km)
1 km AVHRR (entire region)	18.3	3.8	10.3	232.4	9.0
1 km AVHRR (flight track)	18.7	2.3	9.6	228.7	9.5
4 km AVHRR	19.7	3.9	6.8	226.6	9.8
4 km GOES 20.75 UTC	17.9	2.1	4.3	230.9	9.2
MASP 20.55 - 20.61 UTC	18.7	1.9	-	-	-
MASP 20.43 - 20.49 UTC	19.6	2.7	-	-	-
PVM 20.55 - 20.61 UTC	11.8	1.6	-	-	-
PVM 20.43 - 20.49 UTC	12.7	2.1	-	-	-

Table 2. Summary of derived cloud properties from wave cloud, April 30, 1996.

Data	D_e (μm)	$\sigma(D_e)$ (μm)	Optical Depth	Cloud Temperature (K)
1 km AVHRR (entire region)	19.8	5.4	6.4	252.5
4 km AVHRR (e > 0.75)	23.4	8.8	4.0	256.8
4 km AVHRR (e > 0.90)	20.8	3.9	5.7	255.4
4 km GOES (e > 0.75)	22.8	9.9	2.7	259.7
4 km GOES (e > 0.90)	14.2	1.1	5.6	259.7
MASP (20.0 - 20.8 UTC)	16.2	3.0	-	-
MASP (20.8 - 21.5 UTC)	14.7	2.1	-	-
PVM (20.0 - 20.8 UTC)	17.1	2.9	-	-
PVM (20.8 - 21.5 UTC)	16.9	2.4	-	-

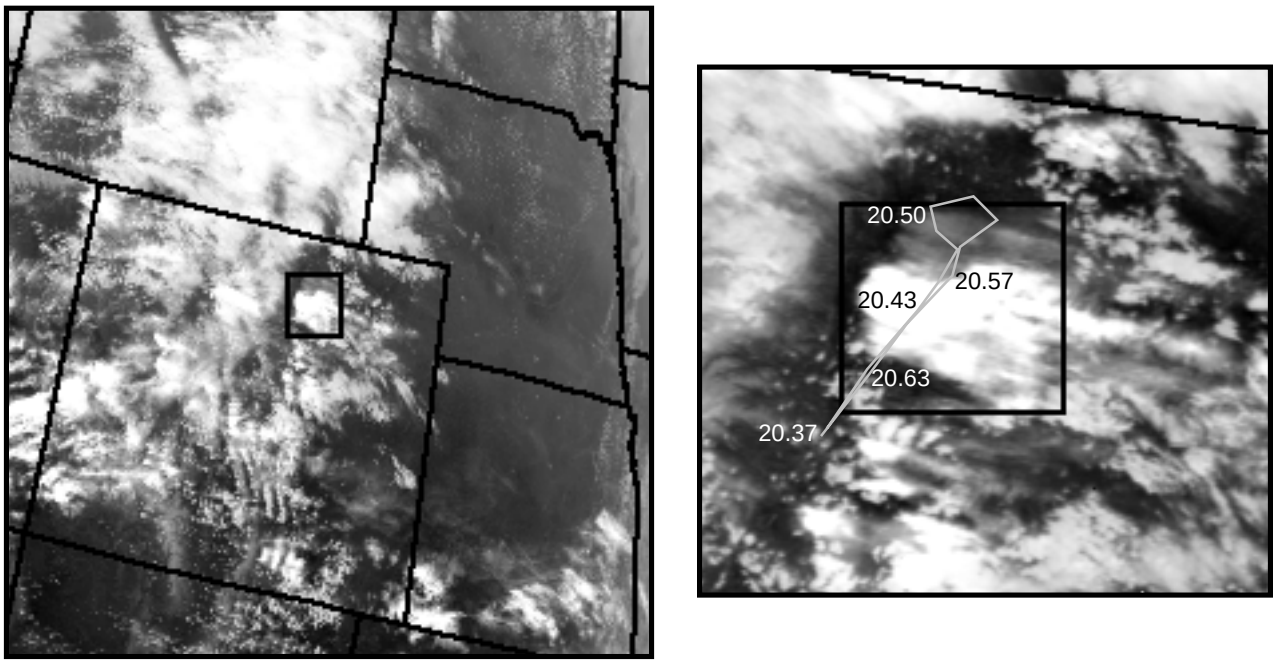

Figure 1. AVHRR IR imagery of the wave cloud over Colorado, 20.56 UTC, May 2, 1996. The enlarged image on the right shows the DC-8 flight track for 20.37 - 20.65 UTC

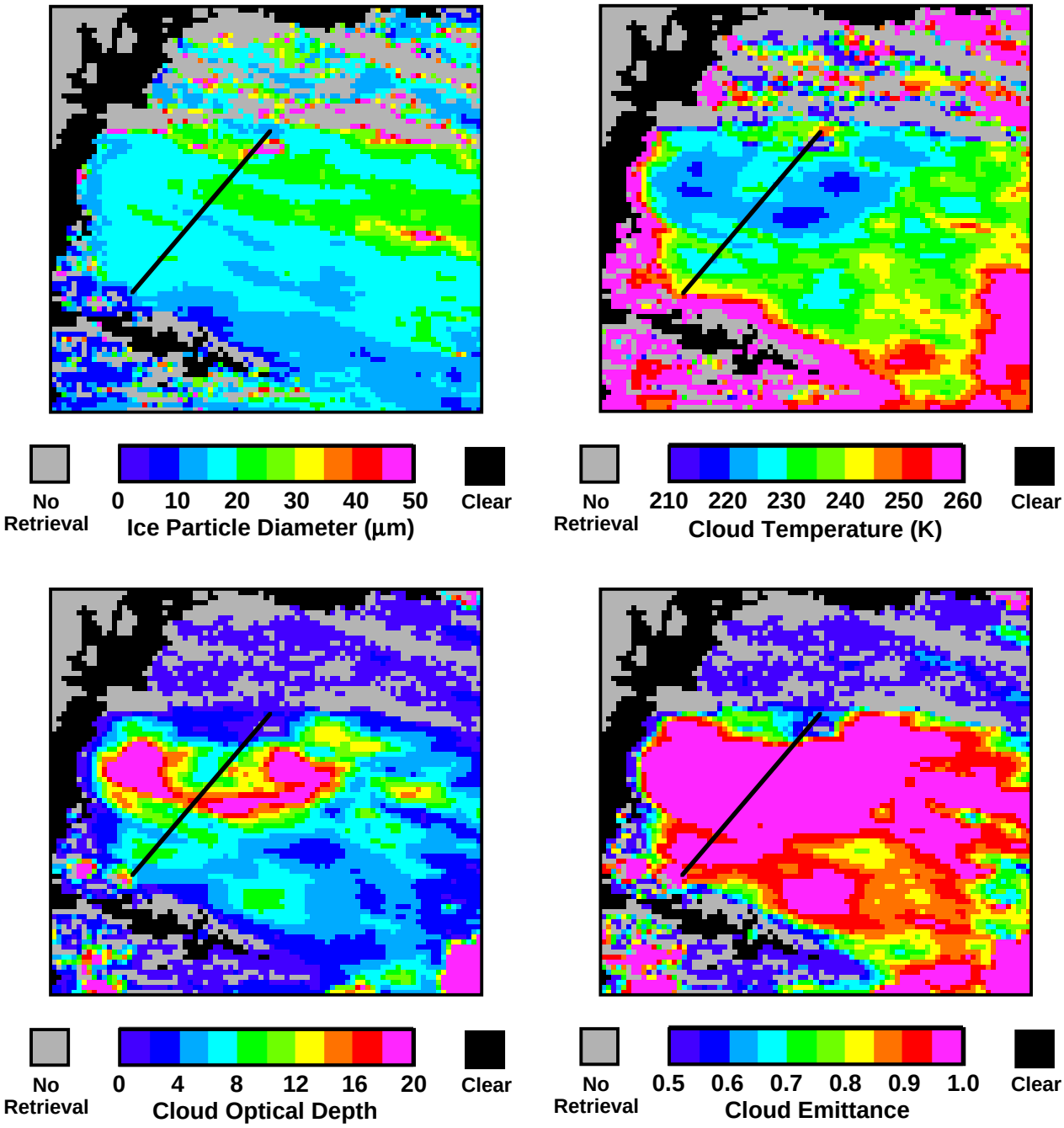

Figure 2. Cloud properties retrieved using VIST from 1-km AVHRR data, 20.56 UTC, May 2, 1996. The region corresponds with the box in Figure 1. The solid line indicates the location of the DC-8 flight track from 20.55 - 20.61 UTC.

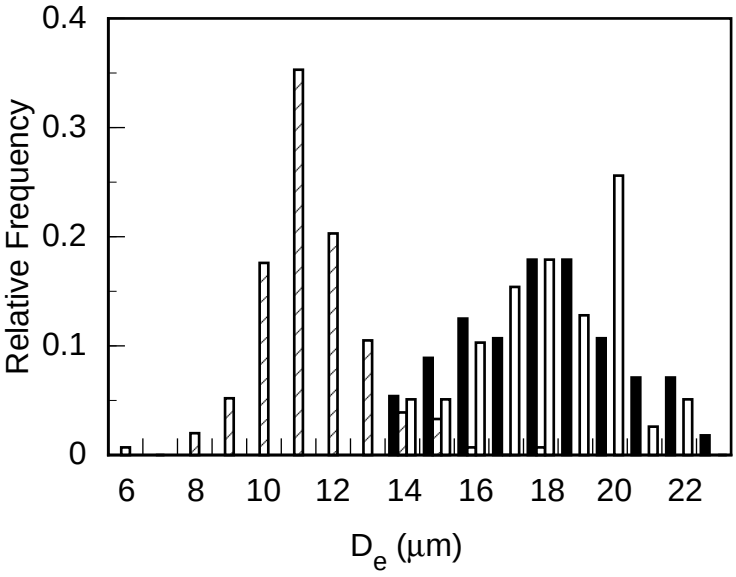

Figure 3. Comparison of the distribution of effective ice particle diameters derived along the DC-8 flight track on May 2 from VIST (black), MASP (white) and PVM (hatched).

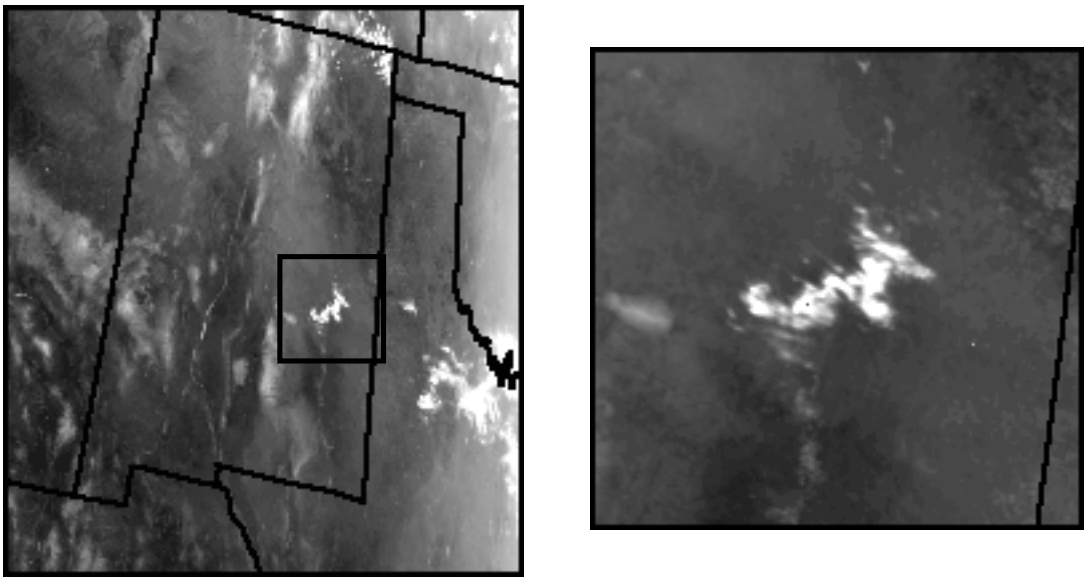

Figure 4. AVHRR IR imagery of the wave cloud over New Mexico, 20.92 UTC, April 30, 1996. The image on the right shows the 1-km data for the area in the box.

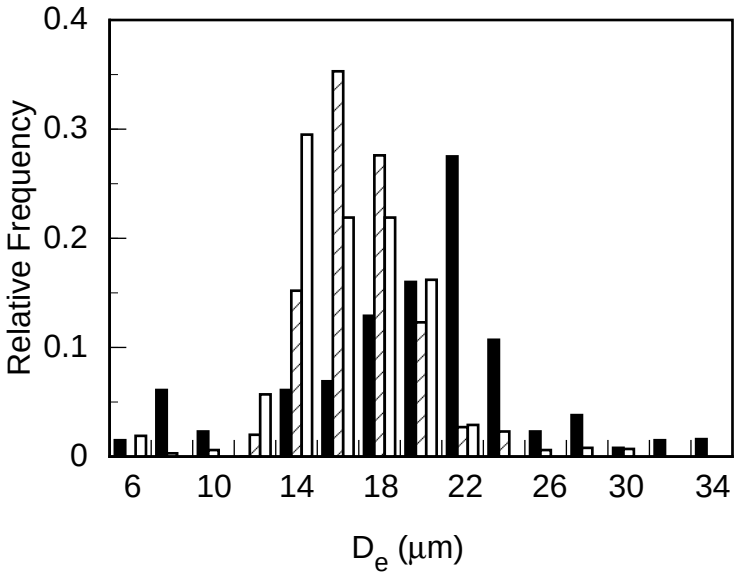

Figure 5. Comparison of the distribution of effective ice particle diameters derived in the April 30 wave cloud from VIST (black), MASP (white) and PVM (hatched)